



Sedimentology, sequence stratigraphy and their control on reservoirs quality in mid-Cretaceous Mishrif formation in East Rub al Khali Basin, Western UAE

Congsheng Bian¹ · Tao Yang¹ · Qingchun Zhang¹ · Mingsheng Lv² · Yongxin Li¹ · Gang Liu¹ · Haigang Duan¹ · Beiwei Luo¹ · Xinshun Zhang¹ · Qingyu Huang¹ · Peiguang Yang¹ · Shuyuan Shi¹ · Jing Zhang¹

Accepted: 8 September 2022 / Published online: 23 September 2022
© The Author(s), under exclusive licence to Springer-Verlag GmbH Germany, part of Springer Nature 2022

Abstract

The Cretaceous Mishrif Formation in the west UAE, East Rub al Khali Basin has got new discoveries; however, there is a lack of systematic and detailed research on the sedimentology, sequence stratigraphy and reservoir distribution of Mishrif Fm. Based on large amount of core and thin section observations, well logging and seismic interpretation, the sedimentary facie association, sequence stratigraphy, and sedimentary evolution of the Mishrif Formation are studied. Moreover, the distribution law and quality of the reservoir are characterized and evaluated. A set of platform carbonate rocks deposited as the Mishrif Formation in the research area, and five typical facie associations are recognized, including rudist-bearing reef, grain shoal, inter-shoal channel/hollow and fore-shoal slope. On this basis, a comprehensive sedimentary evolution model is established. The Mishrif Formation is interpreted as three third-order sequences and six forth-order sequences. In SQ1 and SQ2 sequences, a set of rimmed platform deposited, and ramp deposited in SQ3. Multi-stage platform margins and rudist-bearing reefs develop in HST (highstand systems tract cycles), and successively progradation to the Shilaif sub-basin in the east. The Mishrif reservoir is mostly composed of rudstone, grainstone, and packstone, with well-developed intergranular and dissolved pores. The total porosity reaches above 20%, and the permeability is 1–100 md. The reservoir quality is strongly controlled by facies' associations and dissolution near sequence boundaries. Reef-shoal reservoirs near sequence boundaries in top of HST have higher porosity and permeability than those in other facies belts and position of sequence.

Keywords Face association · Sequence stratigraphic · System tract · Carbonate reservoir · Mishrif formation · East Rub al Khali Basin, west UAE

Introduction

Mid-Cretaceous Mishrif Formation was formed in the passive continental margin during the development of Neo-Tethys Ocean. It is widely distributed in the Middle East, and is composed of shallow-water carbonate platform depositions (Sharland et al. 2001; Ziegler 2001). The formation is rich in rudist fossils (Aqrabi et al. 1998), and it is an important hydrocarbon-bearing formation in the Middle East.

Many oil and gas reservoirs, located in several countries, have been found in the Mishrif Formation in Mesopotamia Basin, Rub al Khali Basin, and Oman Basin. Several large oilfields in Mishrif Formation have been discovered in Iraq, such as Rumaila, Halfayah, and Zubair, and their reserves exceeds more than 30% of the total proven reserves in Iraq (Aqrabi et al. 2010; Mazeel 2012). Recently, high-quality thick reservoirs have also been discovered in Mishrif Formation in west UAE, East of Rub al Khali Basin, which shows its great exploration potential. Up to now, Mishrif Formation has been an important exploration field in the Cretaceous strata of study area.

Carbonate platform reservoirs are globally distributed in the Paleozoic and Mesozoic strata (John and Zuwaina 2014; Philippe et al. 2014). Platform carbonate reservoirs and reef-shoal reservoirs bear large amount of oil and gas reserves, such as the Dengying formation of Sinian and the

✉ Congsheng Bian
biancongsheng@126.com

¹ PetroChina Research Institute of Petroleum Exploration and Development, Beijing 100083, China

² China National Oil and Gas Exploration and Development Corporation Ltd, Beijing 100034, China

Longwangmiao Formation of Cambrian in Sichuan Basin (Zou et al. 2014; Du et al. 2014), the Changxing Formation of Permian (Hong et al. 2008; Ni et al. 2007), the Carboniferous formations in Marginal Caspian Basin (Paola et al. 2010), and the Jurassic-Cretaceous formations in Arabian Basin (Mahdi et al. 2013; Aqrabi et al. 2010). Previous studies showed that the development of platform carbonate reservoirs is controlled by various factors such as depositional environment, sedimentary facies, platform types, diagenesis, especially the distribution of sedimentary facies and diagenesis under the sequence stratigraphic cycles (Aqrabi et al. 1998; Cantrell et al. 2020; Li et al. 2020a, b).

The platform carbonate reservoirs of Cretaceous in the Middle East is young and shallow-buried, resulting in weak diagenesis compared to that of the Paleozoic and Early Mesozoic reservoirs. Recrystallization, especially dolomitization, is weaker in the Cretaceous reservoirs. The quality of reservoirs are generally controlled by its original sedimentary facies and subsequent diagenesis. Aqrabi suggested that the reservoirs in Mishrif Formation in Iraq are mainly composed of rudist-bearing rudstone and packstone, and its porosity is greater than 20% (Aqrabi et al. 1998). Yu and Canrell pointed out that the reservoirs in Mishrif Formation in the south Iraq are mainly composed of high-energy shoals and rudist build-ups, and their porosity and permeability was improved by dissolution when exposed in LST (low stand system tract; Yu et al. 2018; Cantrell et al. 2020). Therefore, it is particularly important to study the distribution and evolution of sedimentary facies based on petrology and sequence stratigraphy for the Mishrif Formation reservoirs in the Middle East. The distribution of high-energy facies such as reefs and shoals determines the development range of favorable reservoirs. However, up to now, the research on Mishrif sedimentary reservoirs in the Middle East has mainly focused on Iraq area of Mesopotamia basin (Mahdi and Aqrabi 2014; Aqrabi et al. 1998, 2010). There is seldom research on the Mishrif Formation in Rub al Khali basin, which is not only lack of systematic and detailed study on the sedimentary characteristics, platform types and sedimentary facies distribution, but also the differences and changes of Mishrif Formation in this area compared to it's in the Mesopotamia basin. It brings important challenges to the oil and gas exploration of Mishrif Formation in Rub al Khali basin.

The depositional environment of Mishrif Formation in the east Rub al Khali Basin is similar to that in Iraq, and some oil reserves have been discovered here recently. However, further hydrocarbon exploration in this area is difficult due to large variability of the depositional facies belts vertically and laterally. The distribution law of favorable microfacies is also unclear (Deng et al. 2016). Therefore, to solve these problems, core and thin section observations, porosity and permeability measurements, and diagenetic analysis were

completed with the help of analytical instruments such as microscope, cathodoluminescence, and mercury injection. On this basis, rock types and sedimentary facies combination of Mishrif Formation in the study area are clarified, the distribution and evolution model of sedimentary facies under the sequence framework are established, and the control factors and distribution of reservoir development are discussed. This paper provides an important reference for the study of sedimentary and reservoir characteristics of Mishrif Formation in Rub al Khali basin, and the technical support for oil and gas exploration in this area.

Geologic setting

The study area is located in the northeast of the Rub al Khali Basin between the Qatar-Fars uplift and the Oman Mountains, which is generally a stable syncline structure (Fig. 1; Ali and Watts 2009; Ali et al. 2013; Bian et al. 2022). The tectonic activity in the study area is weak, only developing inherited monoclinic structure plunging toward southeast, the center of the Shilaif basin. Some faults and nose structures along north–south or northeast directions developed successively from west to East during the Mishrif Formation deposition.

The depositional environment of Cretaceous in the research area was shallow carbonate shelf, which lasted since the Late Permian. In the early Cretaceous, Thamama Group was deposited in this area by ramp deposits with thick and homogeneous packstone and wackstone (Sharland et al. 2001). At the beginning of Aptian, the research area showed obvious regional sedimentary differentiation. Basin-facies mudstone and argillaceous limestone deposited in the northeast of UAE, and rimmed carbonate platform reef-shoal limestone deposited around the Bab Basin in the middle and southwest of UAE, constituting the Shuaiba formation (Mohammed 2020; Jean et al. 1998). The reef-shoals deposited in the ramp and rimmed platforms of early Cretaceous are the main oil-bearing reservoirs, characterized by wide distribution, large thickness and regional stability (Ehrenberg 2019; Ehrenberg et al. 2020). In Albian age of early Middle Cretaceous, the Arabian Shield is eroded, and the mudstones and siltstones of Nahr umr Formation deposited in the research area and surrounding areas (Amer 2015), which was ended by the rapid, extensive transgression in late Albian, and the ramp deposited in Muddud Formation. In the early Cenomanian, the transgression continued in the whole region, and the basin-facies mudstone deposited as Shilaif Formation. Subsequently, with the gradual descending of sea level, carbonate platform deposits constituted the Mishrif Formation in the east part of research area, the basin-facies sediments continually deposited in the southeast part, and reef or shoal developed in the high-energy facies (Fig. 2).

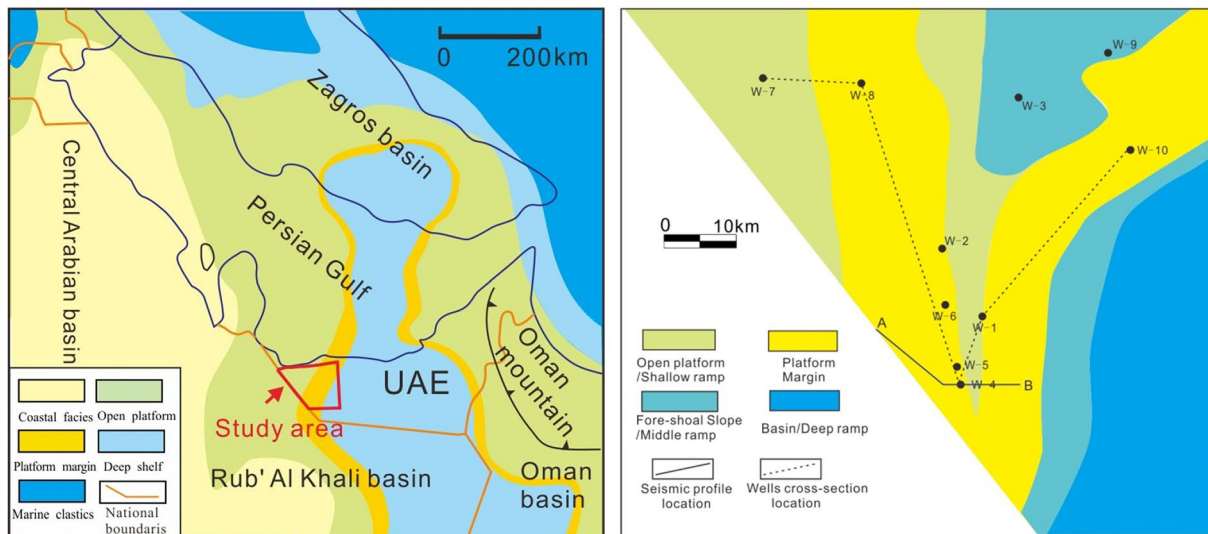


Fig. 1 Location (left) and Sedimentary facies map (right) of Mishrif Formation, mid-Cretaceous in study area, Eastern Arabian plate. *Note.* The Sedimentary facies map (right) of Mishrif Formation is

In the late Cenomanian, regression happened widely in the research area, and Tuwayil sandstones and mudstone deposited as thin layers above the Mishrif Formation. In the end of Cenomanian age, the transgression returned, and a set of shallow carbonate platform deposited as Ruwaydha Formation, which is similar to that of Mishrif Formation. In the early Turonian, sea level descended in the whole area, and an extensive erosion lasted for nearly 4 Ma until the Middle Cretaceous (Alsharhan 1995a).

The thickness of Mishrif Formation in research area is about 300–400 m, and can be divided into three sections vertically according to changes characteristic of lithology, physical properties and logging curve. Reservoirs are distributed in all the three sections, but oil accumulations are mainly discovered in the upper section. Drilling reveals rudist carbonate platform deposits in Mishrif Formation in west area, while the slope-basin facies seposits in east part of research area (Figs. 1, 2).

Data and methods

Data collection in this research contains 540 ft. core samples in four wells, over 150 thin sections, more than 200 measurements of porosity and permeability, well logs of 10 wells, 2D seismic profiles, and 3D seismic volumes (Table 1). Based on lithological classification (Dunham 1962), platform classification (Wilson 1975), and facies pattern classification (Flügel 2006), the color, structure, mineralogy, and biology of the core samples were studied to characterize the reservoir lithology. Log curves and seismic volumes were used

based on the result of this study, and it is a integration diagram of the three members of Mishrif Formation

to establish the facies combination. Based on the sequence stratigraphic principles and research methods of Vail (1988) and Wagoner (1995), the distribution of third-order and fourth-order sequences and system tracts were interpreted using sedimentary facies, log curves, and the distribution of seismic facies. Based on thin sections observation, porosity and permeability measurements, and cathodoluminescence, the pore types, diagenesis, and pore structures of the Mishrif deposits were analyzed, and the controlling factors and distribution law of high-quality reservoirs were generalized.

To determine the microscopic pore characteristics of limestone in Mishrif Formation, polarizing microscopes were used to observe and make statistics on minerals and pores from 4 wells, and the Mercury Injection Capillary Pressure (MICP) method was adopted to analyze the porosity and pore structure characteristics in the study area. Moreover, Cathodo luminescence microscope is used to observe limestone digenesis process and types.

Results

Lithology and sedimentary facies associations

Based on core and thin section observations, and references of neighboring areas (Aqrabi et al. 1998, 2010; Cantrell et al. 2020), it is concluded that the reservoirs in the research area are mainly composed of limestones. The rock compositions, contents of bioclasts, and the types of cements, however, vary greatly in different well sections and areas, and can be mainly classified into five combinations.

Fig. 2 Chronostratigraphy of stratigraphy and Supersequence of Cretaceous in study area (Altered after Sharland et al. 2001)

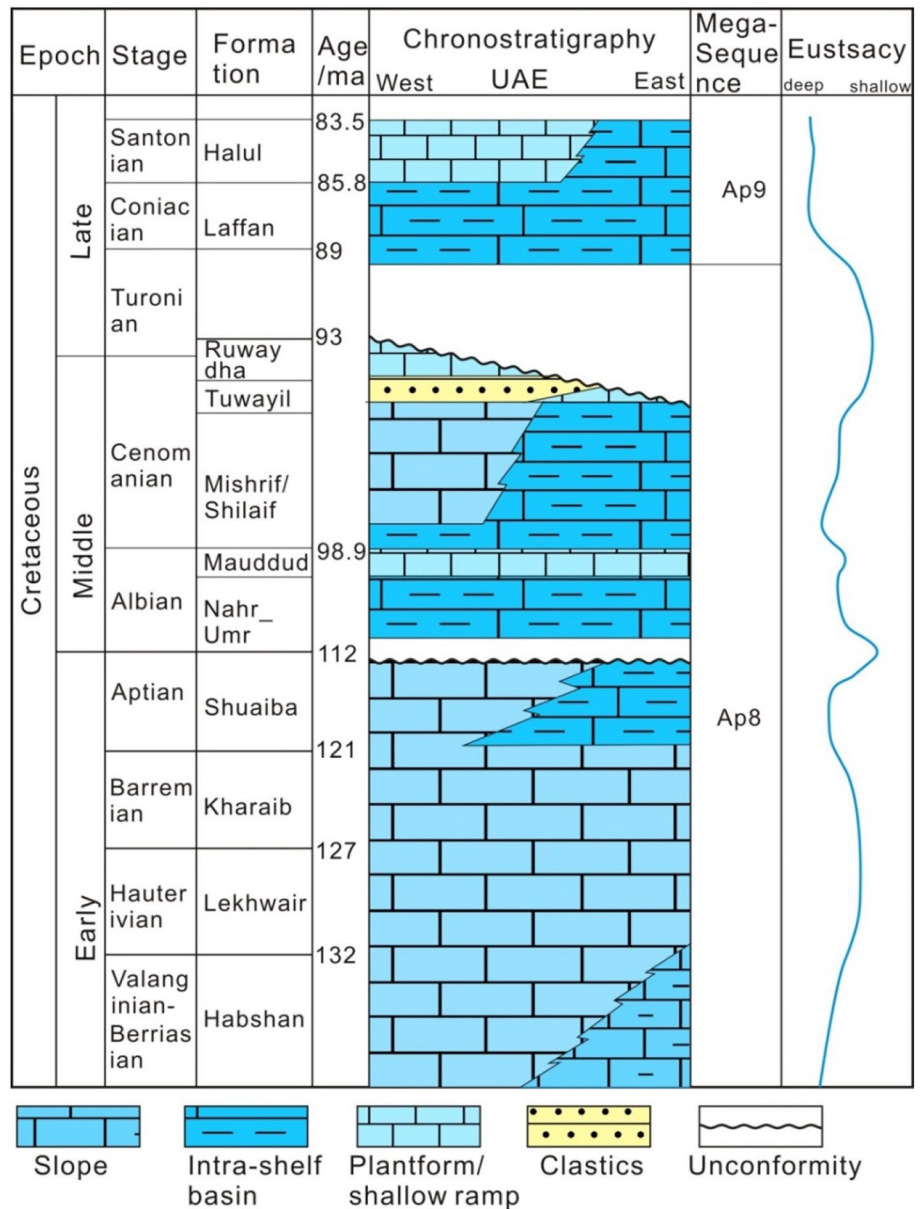


Table 1 Cores, thin section and well logging description of 10 wells in study area

Well	Core	Thin section	Well Logging
W-3	90 ft., in the top of Mishrif Formation , gray to dark gray, with nodular or lenticular shapes	30 slices, Lithology is mainly wackstone and mudstone, with small part of muddy limestone	GR, DT, RT
W-4	90 ft., in the top of Mishrif Formation , including 5 ft. of Tuwayil Formation, grayish white to gray	18 slices, Lithology is mainly Rudstone, Packstone and small amount of wackstone, with plenty of rudists and bivalves bioclasts	GR, DT, RT
W-5	180 ft., in the top and lower part of Mishrif Formation , including 7 ft. of Tuwayil Formation, grayish white to gray	52 slices, Lithology is mainly Rudstone, Packstone with plenty of rudists and bivalves bioclasts	GR, DT, RT
W-6	180 ft., in the top and lower part of Mishrif Formation , including 12 ft. of Tuwayil Formation, gray to dark gray	55 slices, Lithology is mainly Packstone, wackstone, and small small amount of wackstone, vertical boring and burrowtion structure developed	GR, DT, RT

These combinations reflect the variation of sedimentary environments.

Rock types of Mishrif Fm

According to the Dunham classification (1962), the reservoir rocks in Mishrif Formation can be classified into rudstone, grainstone, packstone, wackstone, and mudstone (Figs. 3, 4). The rudstone is mainly composed of rudist framework, bioclasts, and sparry cements. The rudist frameworks are well preserved in most cases, and their diameters are about 0.5–3 cm. These frameworks are filled with calcite cements, and dissolution pores developed. Bioclasts and sparry cements filled the spaces between the frameworks, in which the bioclasts are almost rudist fragments (Figs. 3a, 4a, b). Core sample observations reveal that the rudstone is mainly distributed in the upper and lower part of the Mishrif Formation with multi layers, and the thickness of a single layer is 0.5–1 m.

The grainstone is mainly composed of gray to light-gray bioclasts and sparry cements, belonging to leucoclastic limestone. The bioclasts is composed of rudists and bivalves, and its content is over 70%. Intergranular and dissolved pores are observed in grainstone, with cross beddings developed often. Vertically, grainstone interbeds with the rudstone in the middle-lower and top part of the Mishrif Formation (Figs. 3b, 4c, d).

The packstone is mainly composed of grains and micrite-microcrystalline calcites, belong to Micritic bioclastic limestone. The grains are mainly composed of bioclasts, whose content is over 50%, and are constituted by rudists and other bivalves, echinoderms and foraminifera. The packstone shows poor sorting, certain rounding, inter- or intra-granular dissolution pores. Inside the packstone a large amount of boring pores and bioturbation structures, and the micrite envelope of grains, indicate low energy of water body. Packstone is widely distributed, and has higher content compared to other rock types in Mishrif Formation (Figs. 3c, 4e, f).

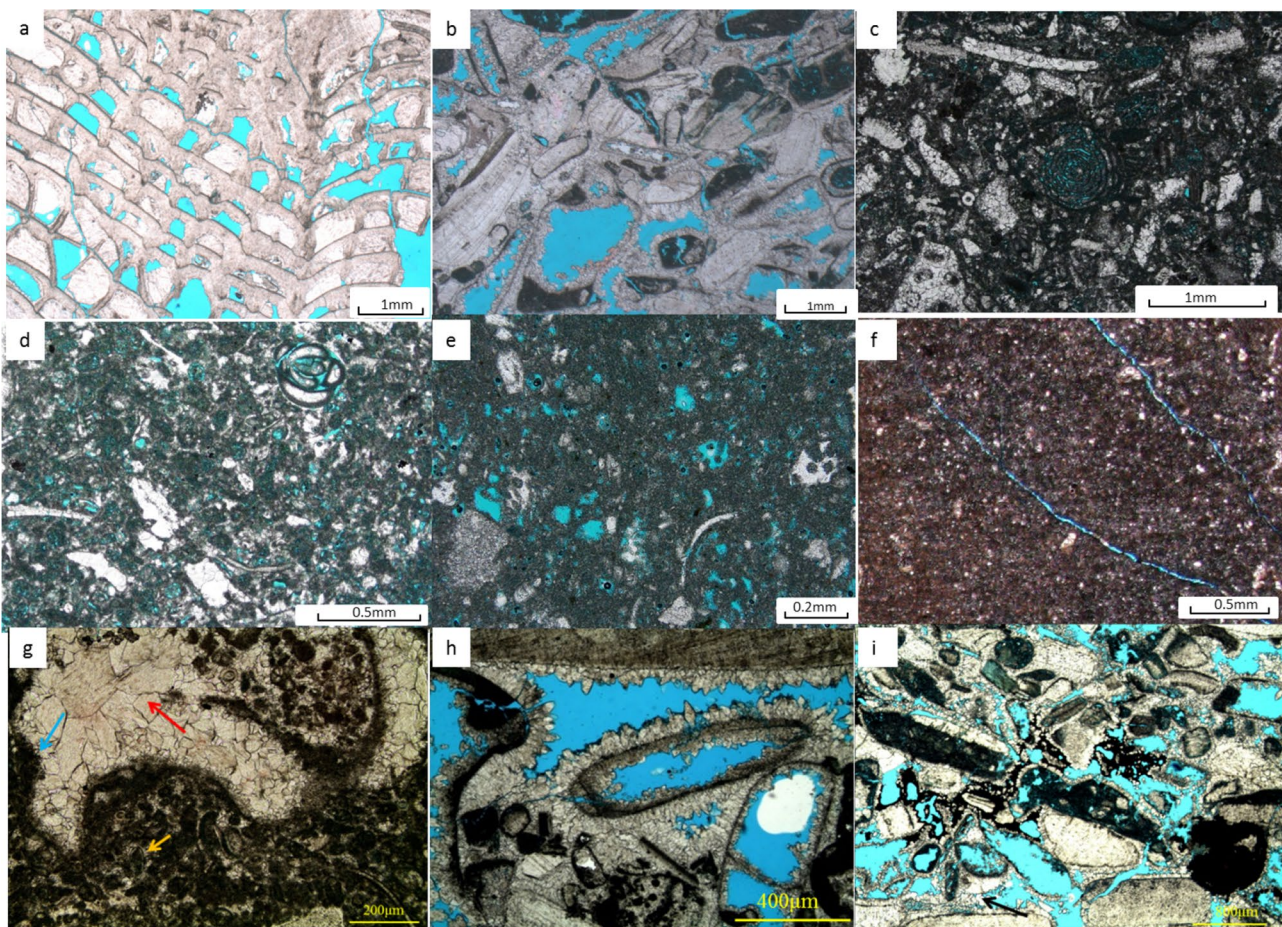


Fig. 3 Photomicrographs of rocks, pore and diagenesis features of Mishrif Formation in study area. **a** Rudstone, W-5 well, 6223.2f; **b** Grainstone, W-5 well, 5625.5 25 ft.; **c** Packstone, W-6 well, 5453.17 ft.; **d** Packstone, W-6 well, 5384.15 ft.; **e** Wackstone, W-6

well, 5459.2 ft.; **f** mudstone, W-3 well, 5799.1 ft.; **g** Packstone, W-6 well, 5382.2 ft.; **h** Grainstone, W-5 well, 5589.45 ft.; **i** Grainstone, W-5 well, 5634 ft.)

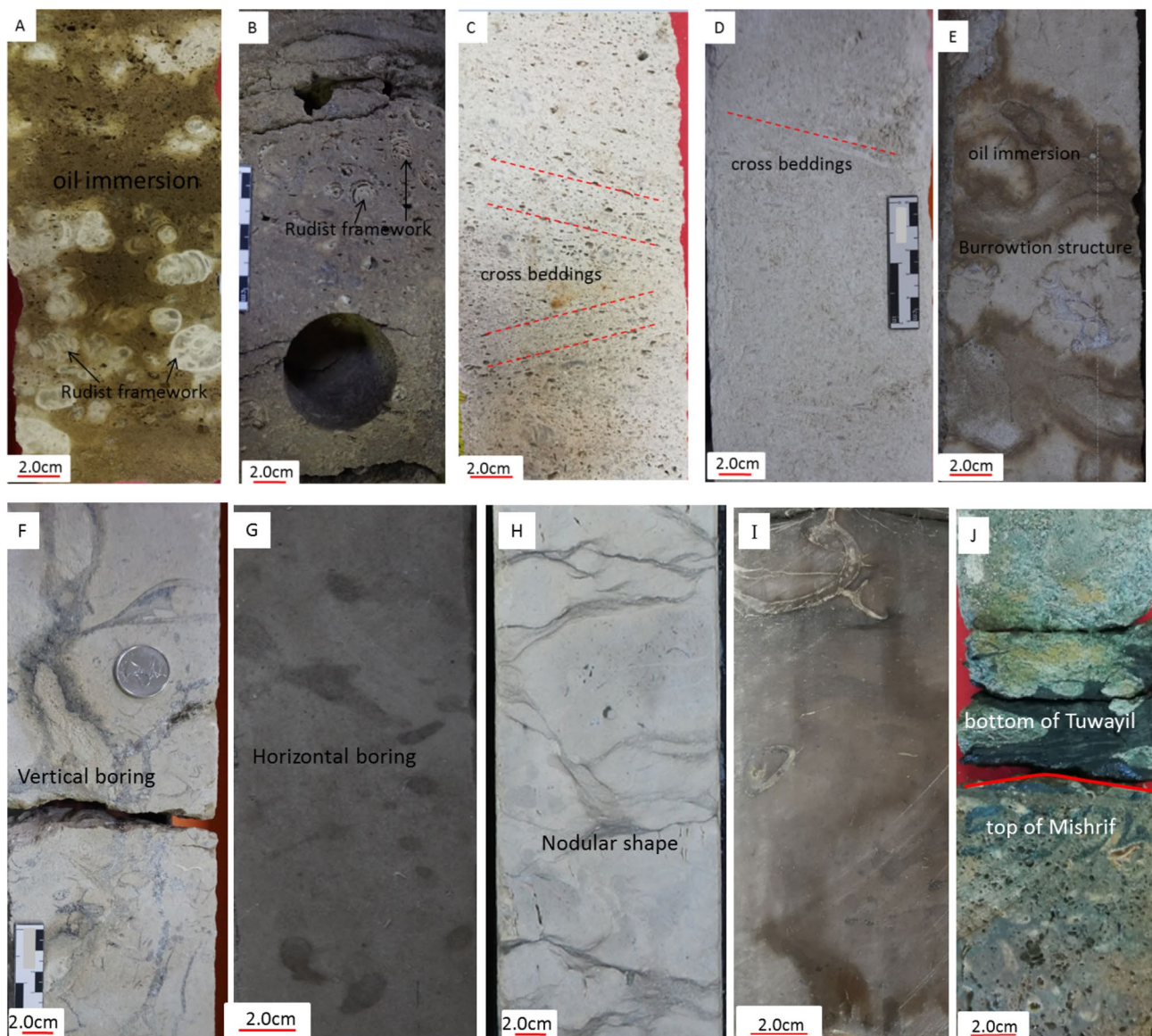


Fig. 4 Core photographs of different types Facies associations of Mishrif Formation in research area. **a, b** Rudist-bearing reef, Rudstone bearing plenty of rudist frameworks and its clasts, oil immersion, W-4/W-5 well, 5598/5595 ft.; **c, d** Grain shoal, mainly grainstone, bearing plenty of rudist and bivalves clasts, with low-angle cross beddings, W-4/W-5 well, 5646/6295 ft.; **e, f** Inter-shoal channel, mainly Packstone, bearing a large number of nearly vertical burrows,

with oil immersion, W-6/W-5 well, 5417.4 ft./5644 ft.; **g** Inter-shoal hollow, mainly wackstone, with nearly horizontal burrows, W-6 well, 5478 ft.; **h** Fore-shore slope, mainly mudstone and wackstone, with lenticular shapes, W-3 well, 5751 ft.; **i** Slope or basin, muddy limestone, massive, occasionally with bio-detritus, W-4 well, 7062 ft.; **j** Boundary of Mishrif and Tuwayil Formation, W-4 well, 5994 ft.)

The composition of wackstone is similar to that of packstone, but its grain content is usually below 50%, belonging to bioclastic micrite limestone. The wackstone shows small grain size and poor sorting. The types of bioclasts of wackstone are the same with that of packstone, while the contents of echinoderm and foraminifera are higher. The contents of micrite calcite in cements is high, and a small amount of inter- or intra-granular dissolution

pores developed (Figs. 3d, 4g). The gray to dark gray mudstones are mainly composed of microcrystalline calcites with high lime mud content, forming medium-thin layers. Very small amounts of bioclasts and pores are observed in the mudstone. The mudstone mainly formed in the deep-water condition in the east of the basin; their distribution is limited in the research area (Figs. 3e, f, 4h).

Facies associations

Based on core and thin section samples and logging in four wells, five typical facies combinations, including rudist-bearing reef, grain shoal, inter-shoal channel, inter-shoal hollow and fore-shore slope were identified (Fig. 2) through the detailed study of facies. Further, recognition criterion in core samples, thin sections, and well logging for each combination were established (Figs. 4, 5, 6).

Rudist-bearing reef The rudist-bearing reef is composed of biological framework and bioclasts. The biological framework are mainly constituted by rudists and a small number of bivalves and gastropods. The lithology is mainly gray to gray-white rudstone and grainstone. Biological frameworks and bioclasts can be seen in the core samples; their length is 3–10 cm, mainly 0.5–2 cm. The biological frameworks are mostly shaped as arc and horn, showing irregular arrangement and poor sorting. Fibrous-like textures with dark and light stripes are observed under microscope, as well as

Fig. 5 Typical sedimentary facies lithology and response on wireline logs of the Mishrif Formation

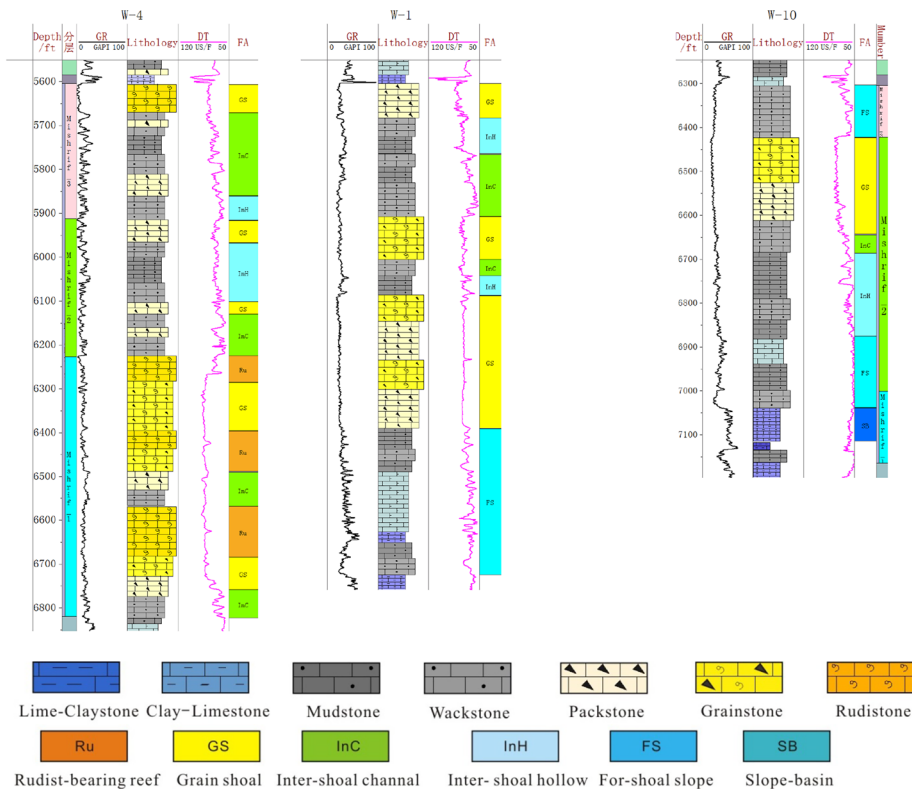
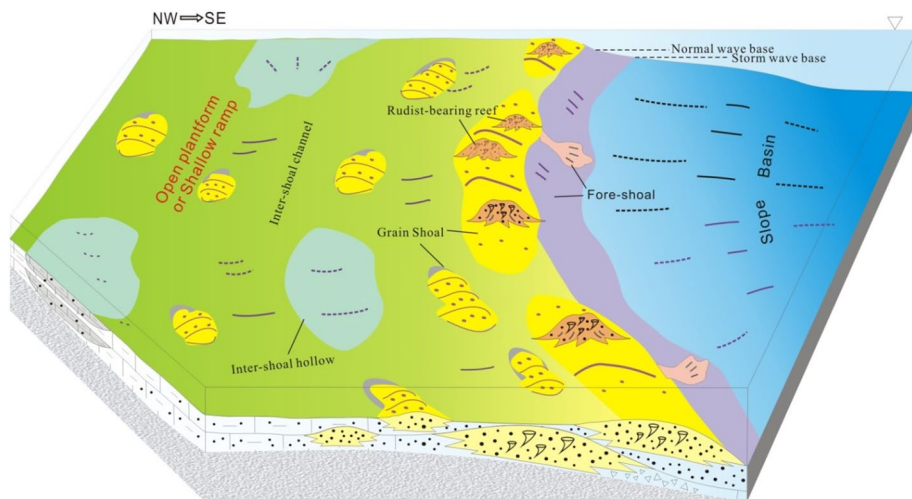


Fig. 6 Distribution model of the facie associations in Mishrif Formation



the relatively complete rudist frameworks. Rudist-bearing reef is usually composed of interbedding of rudstone and grainstone; the thickness of a single layer is 3–10 ft., and the whole thickness of the layer series reaches 10–30 ft. (Fig. 4a, b). Logging curves of the rudist-bearing reef show a box-like shape with great thickness, and its low GR value (0–10 API) and high DT value (75–90 $\mu\text{m/s}$) indicate low lime mud content and good reservoir properties (Fig. 5). The rudist-bearing reefs are mainly distributed on platform margins and in shallow ramp facies (Fig. 6).

Rudist is widely distributed and main reef building organisms in the Cretaceous period, and died out at the end of the Cretaceous (Philip and Airaud 1991; Malte and Parente 2008a, b; Alsharhan 1995b). Research shows that the rudist has only one shell top attached to the base due to its special structure, and its stability is poor. During its growth, it is easy to be damaged by waves and ocean currents. Therefore, it is difficult for the rudist to develop large and complete reefs. Generally, the thickness of single layer rudist reef is thin, and the thickness of longitudinal layers is large. In the study area, the thickness of the whole rudist-reef layer is relatively thin, which is about 1 m, while the grainstone composed of rudist framework debris is relatively more developed and the arrangement is irregular, which is different from the typical reef like coral reef.

Grain shoal The grain shoal is mainly formed by gray-white to gray grainstone and packstone, filled with high content of micrite and low content of lime muds. The contents of bioclasts in grain shoal are similar to or lower than that in the rudist-bearing reef, but short of complete rudist framework. The main type of organisms is rudist, along with a few gastropods, echinoderms, and foraminifera. Some thin layers of grain lime mud are highly cemented and few pore space is preserved. Inclined bedding and cross bedding are observed in the core samples of grain shoal (Fig. 4c, d). In logging profiles, grain shoal shows zigzag curves, and are characterized by low and stable GR (10–25 API), and middle-high DT (65–85 $\mu\text{m/s}$), indicating variations in lithology and lime mud content vertically. The thicknesses of a single layer in grain shoals typically are 2–6 ft., and the cumulative thicknesses of layer series usually adds up to 10–50 ft. (Fig. 5b). Grain shoal are mainly distributed in the platform margin, shallow ramp, and open platform facies (Fig. 6).

The bedding structure in the grain shoal indicates the reconstruction and transportation of sediments by strong wave or ocean current. The existence of micrite cementation indicates relatively weak water energy in some grain shoals. The existence of small organisms, such as the foraminifera, also indicates lower energy or greater depth of the water body when grain shoal formed than those of rudist-bearing reef.

Inter-shoal channel The inter-shoal channel develops in the lower terrain between the rudist-bearing reefs or the grain shoals, with gray to dark gray packstone and partly grainstone. The content of bioclasts in the inter-shoal channel is relatively lower than that of grain shoal, and the grain size is smaller. The bioclasts are mainly composed of rudist and gastropod, as well as echinoderm and foraminifera. Vertical boring and burrowtion structure are observed in inter-shoal channels, and mud laminae develop regionally. The rocks in inter-shoal channel is relatively strong cementation, and poor porosity (Fig. 4e, f). In well log profiles it shows middle serrated GR (15–30 API) and middle DT (60–70 $\mu\text{m/s}$), and the thickness of a single layer is 20–50 ft. (Fig. 5C). It is mainly distributed in open platform, shallow ramps, and regional platform margins (Fig. 6).

The increase contents of micrite and lime mud, as well as the development of biological burrowtion structure indicate that the inter-shoal channels are formed in deeper and weaker water bodies. Plenty of the rudist clasts indicates that the inter-shoal channels are located immediately near the rudist-bearing reef or grain shoal.

Inter-shoal hollow The inter-shoal hollow develops in the lower terrain away from the rudist-bearing reefs and the grain shoals, with weaker water energy, smaller grain size and higher contents of lime mud than the inter-shoal channel. The bioclasts are composed of more echinoderms and foraminifera than rudists and gastropods. The rocks are mainly gray to dark gray wackstone, and partly mudstone and lime claystone, with biological horizontal burrow, and argillaceous laminae locally (Fig. 4G). In well log profiles it shows higher serrated GR (30–45 API) and lower DT (55–70 $\mu\text{m/s}$), and the thickness of a single layer is 10–30 ft. (Fig. 5D). It is mainly distributed back of reef or shoal in open platform and shallow ramp (Fig. 6).

The increase contents of clay and lime mud, as well as bentonic clasts indicate that the inter-shoal hollows are developed away from the grain shoal, similar to the position of lagoon. However, the existence of more clasts of rudists and gastropods, and the clay content is not high, which indicates the inter-shoal hollow is different from the typical lagoon (Fig. 4H).

Fore-shore slope The fore-shore slope is mainly composed of gray to dark gray wackstone, a little Packstone and muddy limestone, with nodular or lenticular shapes, and mud laminae developed. Lower content of foraminifera clasts with smaller scales are observed in thin sections, as well as a few echinoderms and small rudist clasts. The rocks of fore-shore slope are highly cemented and show very low porosity (Fig. 4H). Its logging are characterized by serrated meddle-high GR (30–60 API) and low DT (50–65 $\mu\text{m/s}$), and the

thickness of a single layer is 4–20 ft. (Fig. 5E). It is mainly distributed in the up slope and medium ramp facies (Fig. 6).

The mud laminas and foraminifera indicate deep and lower energy water environment of this facies combination, basically below the wave base. But, rudist clasts bearing packstone shows that the fore-shoal slope deposits is not away from the reef and shoal (Fig. 3d). The lenticular and nodular shapes indicate frequent slumping, which often occurs in the ramp or the outer side of platform margin with a large slope angle.

Identification of sequence boundaries and systems tracts

Many previous studies have involved the stratigraphic sequences of the Mishrif Formation in Iraq. Based on the variation of sedimentary facies and system tracts, the Mishrif Formation was divided into three or four third-order sequences (Mahdi et al. 2013; Gao et al. 2013). Based on a comprehensive analysis of core samples, well logs, and seismic data in this area, this research divides the Mishrif Formation into three third-order sequences and six systems tracts (Fig. 7).

The 3rd Sequence boundary

Regional geology and drilling data reveal that the main part of Mishrif Formation in the study area is platform limestone deposit, while the Shiliaf Formation under mishrif belongs to slope to basin facies with claystone or marlite deposit. Their lithology and sedimentary characteristics are significantly different, and the surface between them belonging to the bottom boundary of third-order sequence SQ1. The interface has clear characteristics in lithology, logging and seismic profile (Table 2). The platform facies of Mishrif Formation mainly develops limestone deposits with low or no argillaceous content (Fig. 3a–d), while the shilaif Formation mainly consists of marlite or argillaceous limestone (Fig. 3e). On the logging curve, the natural gamma (GR) and resistivity (RT) curves show a sudden change from high value (35–75 API, 5–80 Ω m) to low value (20–35 API, 0.3–2 Ω m), and the acoustic time difference (DT) curve shows a sudden change from low value (55–65 μ m/s) to high value (70–80 μ m/s; Table 2; Fig. 7). On the seismic profile, a series of features of downlap along the same axis can be seen at the bottom of sequence SQ1 (Fig. 8).

The boundary between SQ1 and SQ2 shows that the sea surface rise from bottom to top, the lime mud content of lithology increase, and the value of GR and RT curve increase from 5 to 15 API and 0.1–2 Ω m to 20–40 API and 5–100 Ω m, respectively (Table 1). On the seismic profile, strong amplitude and parallel reflection are obviously at this interface, and a series of downlap are developed. The

features of transgression onlap are found above the top surface of SQ1 in the East of study area (Fig. 8). The boundary characteristics of sequence SQ2 and SQ3 are similar to those of sequence SQ1 and SQ2, which also show that from SQ2 to SQ3 the sea surface rise, the mud content of limestone increases, the values of GR and RT rapidly increase, and the downlap and onlap characteristics in the seismic profile are also obvious. A regional unconformity exists at the top of the Mishrif Formation, on which the limestone in the core has the characteristics of exposure erosion (Fig. 4J). In seismic profile, the top of Mishrif Formation show a strong reflection waves that can be traced in the whole region, and the interface characteristics are clear (Fig. 8).

The 4th sequence identification

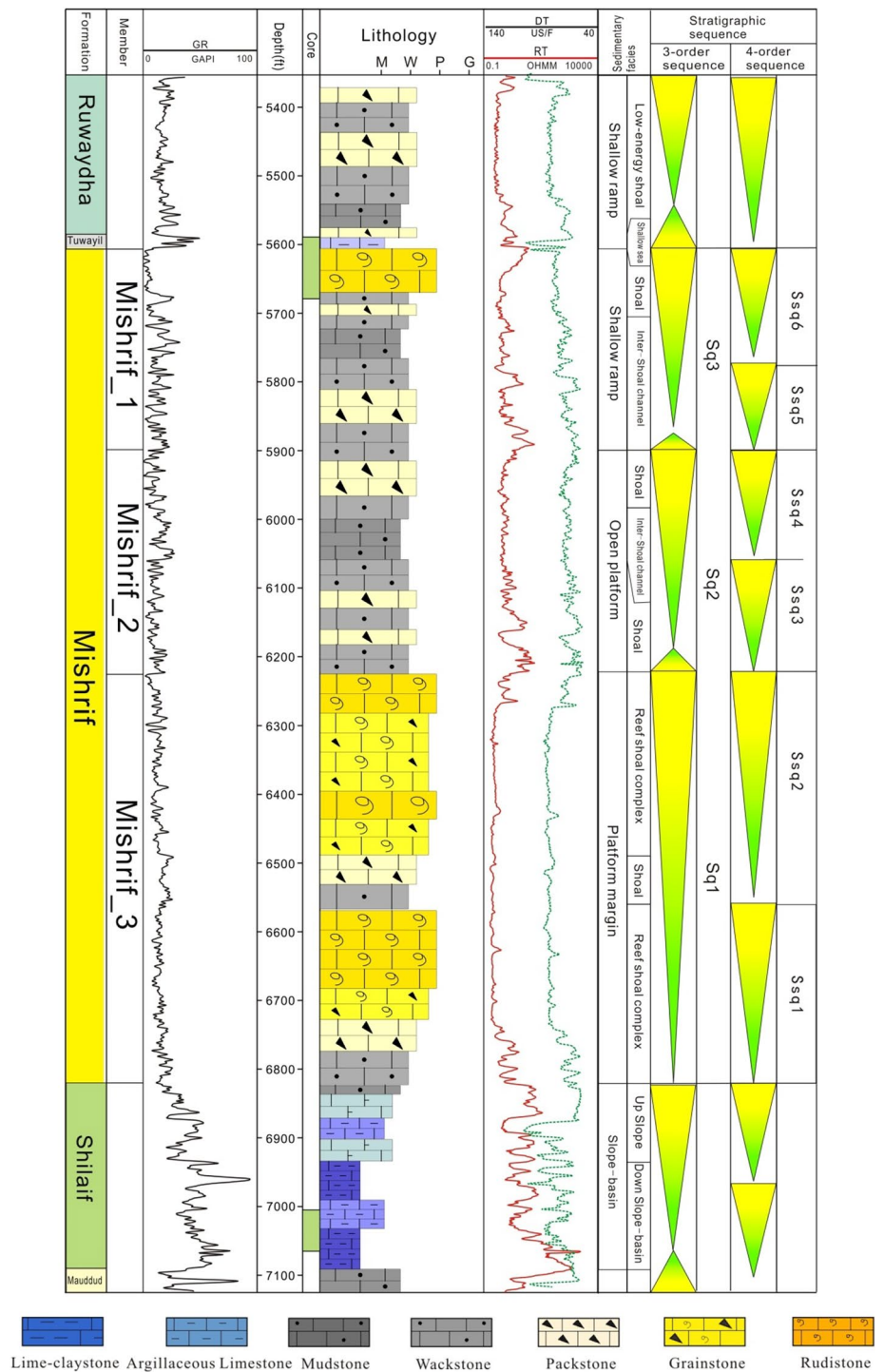
The fourth-order sequence can be identified based on lithology, lithofacies combination, and wave group characteristics in seismic profiles and the maximum flooding surface (Malte and Parente 2008a, b; Alsharhan 1995b; Zhao 2015; Zhang 2017). Through the analysis of lithology and seismic section reflection characteristics in the study area, combined with the characteristics of regional sea level change, it is found that progradation characteristics are mainly developed in the early Mishrif Formation in the study area, and two forth-order sequences (Ssq1–Ssq2) are identified in SQ1, with the thickness of 300 ft. The two forth-order sequences of SQ1 are composed by two highstand system tracts (HST), which are characterized by the sea level dropped down, the value of GR decrease upward, and a sudden change at the interface. The results lead to the increase of water energy, with the increase of bioclasts content and the improvement of reservoir physical properties in the HST of SQ1 (Figs. 7, 8).

The thickness of SQ2 in the study area is only 100 ft., and two forth-order sequences in the platform area are identified with HSTs. However, the values of GR and RT curve in SQ2 are higher than those of SQ1, which means the limestone argillaceous content is higher and the water depth is larger than that of SQ1. Transgressive system tract can be found in the eastern part of the study area (Fig. 8).

(Bian et al. 2022). The maximum flooding surface is characterized by regional distribution of medium-strong amplitude parallel reflection in the seismic profile of Fig. 6, and the HST is characterized by multiple mound reflection of medium-weak amplitude. In SQ3 sequence, there are also two forth-order sequences (TST) in the platform area developed in west-central area, and HST founded just in the east area during early SQ3 showing sea level upward.

(The red and pink dotted line arrows in the figure represent progradation or aggradation of highstand system tracts (HST), and the blue arrow represents transgressive overlap; the pink arrow represents large mound weak seismic reflection, which is confirmed as rudist-bearing reef by W-4

Fig. 7 Chronostratigraphy of stratigraphy and sequence of Mishrif Formation in study area



well core; the red arrow refers to small mound medium-weak reflection, which belongs to grain shoal deposit. The thickness of Mishrif Formation on the right side of the two mound reflection near faults suddenly decreases, which represents the fore-shoal slope facies deposition of the platform margin. In the Mishrif_3 member, there is no thick mound reflection, and the stratum slowly decreases to the right, which represents the ramp deposition; there is a shallow

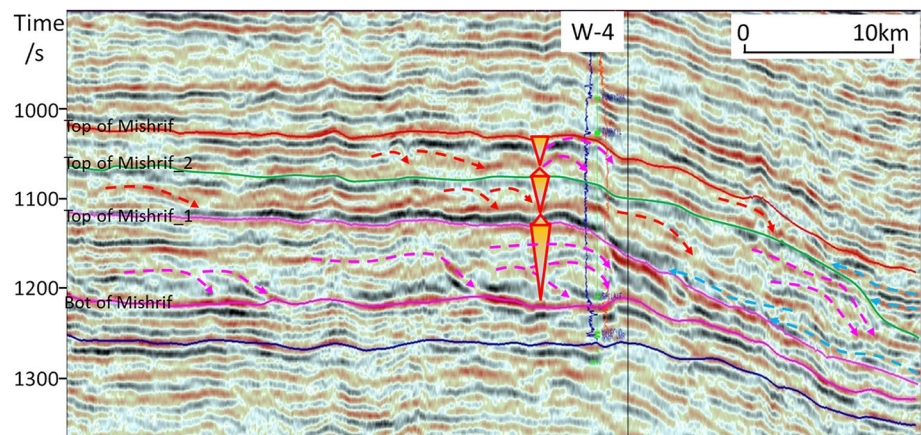
ramp at the well W-4 and its left side, and the thickness decreases to the middle ramp in the right seaward direction.)

Sequence stratigraphic framework and sedimentary facies

Based on data analysis of cores, logging, and seismic, the sequence stratigraphic framework was established by

Table 2 The characteristics of lithology, well logging and Seismic of 3rd sequence in Mishrif Formation

3rd sequence	Lithology	Well logging characteristics			Seismic characteristics
		GR/API	RT/ Ω -m	DT/ μ m/s	
Tuwayil(above of SQ3)	Claystone and sandstone	20–50	65–100	0.5–8	Strong amplitude, parallel reflection
SQ3	Grainstone and packstone, partly rudstone and wackstone	5–15	55–80	0.3–10	Medium and weak amplitude, small mound reflection, downlap
SQ2	Grainstone and packstone, partly wackstone,	5–20	55–75	0.4–5	Medium and weak amplitude, small mound reflection, downlap
SQ1	Rudstone and grain limestone, partly packstone	5–20	75–85	0.2–0.5	Weak amplitude, mound reflection, downlap
Shialif (under of SQ1)	Mudstone marlite	30–90	60–100	6–150	Strong amplitude, parallel reflection

Fig. 8 Seismic section showing facies, stacking patterns and faults of Mishrif Formation in South area (Bian et al. 2022)

the identification of vertical and horizontal third-order sequences in the research area. The east–west connecting-well zigzag profile is perpendicular to the strike of sedimentary facies, and reflects the horizontal changes of the stratigraphic sequence and facies belts (Fig. 9). The profile shows stable distribution of three third-order sequences in Mishrif Formation. The thickness of the lower sequence SQ1 (Mishrif_1) increases from 450 ft. in the west to 550 ft. in the middle part, and then decreases to 200–300 ft. in the east. Two fourth-order sequences (Ssq1 and Ssq2) show same change like third-order sequences in thickness. In the west of well W-4, the seismic reflections show a series of mound prograde reflections with thick layers that gradually migrate toward the sea, while thin strong parallel reflections develop in the east of well W-4 (Fig. 8). In the well profile, big layer of rudstone and grainstone mainly develop in well W-4 and western, and thin layer of wackstone, mudstone, and shale-limestone develop in the east of well W-4. It is concluded that the platform margin developed in the central-west part of study area, and reef-shoal is characterized by the mound build-ups, and the two stages of grain shoal and rudist-bearing reef, migrating and overlying seaward (Fig. 9). The east formation of well W-4 is the slope facies deposits outside the platform margin, which belongs to fore-shoal slope. The

progradation characteristics of HST in SQ1 also exist in the strata of Iran and Oman in the same period (Taghavi et al. 2006; Van et al. 2002).

In the SQ2 period (Mishrif_2), the west formation of well W-4 is mainly characterized by subparallel reflectors with medium-strong amplitude, and small mound reflections that prograde to the sea develop in the middle and upper part of SQ2 (Fig. 8). The east formation of 10 km from Well W-4 is characterized by large mound reflections with weak amplitude that prograde to the seaward, and thin retrograde reflection develop at the bottom of SQ2. The strata thickness of SQ2 also increases from 300–350 ft. in the west to 500 ft. in the middle area, and then suddenly decreases to less than 300 ft. in the east end. In the fourth-order sequence, two HSTs are recognized in the connecting-well profile, while one TST of SQ2 only develop in the lower part of east area. It is concluded that the west and central side of SQ2 of the Mishrif Formation is open platform facies, in which the grain shoal is characterized by weak mound reflections, and the inter-shoal hollow or channel is characterized by medium-strong reflections (Fig. 8). The large-scale mound reflection in 10 km eastern Well W-4 is the complexes of grain shoal and rudstone reef formed in platform margin. There are also two stage reef

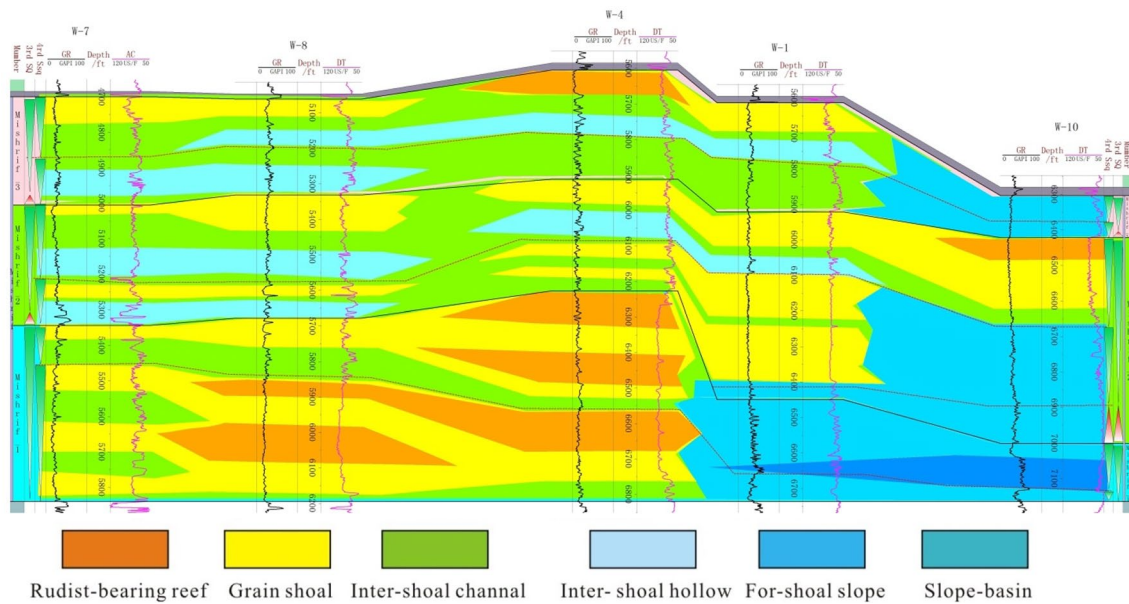


Fig. 9 Sequence framework and sedimentary faces of WE cross-sections through the wells of Mishrif Formation

and shoal deposits progradating to the east which developed in the two HSTs respectively. The retrogress deposits at the bottom of SQ2 was formed in the early stage of TST (transgression system tract). The fore-shoal slope deposits are distributed in the east end of the area beyond the platform margin (Fig. 9).

The stratigraphic pattern of the SQ3 period (Mishrif_3) is similar to SQ2, which contains two HSTs deposits in the forth-order sequence. The features of SQ3 in seismic profiles are similar to those of the open platform in SQ2: subparallel reflections of medium-weak amplitudes and regional small-scale mound reflections. Series of parallel retrogradation reflections only develop easternmost in bottom SQ3 period, and no large-scale mound reflection is observed over SQ3 period (Fig. 8). In the well profiles, the lower HST of SQ3 is dominated by inter-shoal facies, while the upper HST mainly developed shoal and reef, with fore-shoal facies recognized in the east area. The thickness of the formation in SQ3 is relatively stable, with about 300 ft. in the central and west area, and 100–200 ft. in the east (Fig. 9). It is concluded that ramp are the main deposits system in this period. Shallow ramps mainly develop in the central-west part of the research area, where inter-shoal hollows and grain shoal are formed. Middle ramps mainly develop in the east part of the research area. For example, the nodular and lenticular wackstone and mudstone with high argillaceous content are observed in the core samples of Well W-3 (Fig. 4H). No large-scale platform margin is observed in SQ3 formation. The upper part of

the Mishrif Formation was reformed by short-term erosion along with the uplift and expose (Alsharhan 1995b; Hajikazemi et al. 2010; Fig. 4I).

Sedimentary evolution model

The above studies showed that Mishrif Formation in study area developed carbonates platform mainly under regression environment. Three third-order sequences and six fourth-order sequences are recognized in Mishrif Formation, nearly showing reverse cycles upward. With the analysis in seismic profiles, connecting-well profiles, and sedimentary facies, it is concluded that the SQ1 and SQ2 of Mishrif Formation are mainly composed of rimmed platform, and SQ3 is composed of ramp (Figs. 10, 11).

During the SQ1 period, the central-western part of research area was dominated by platform margin facies formed in regression environment. During this period, multi-phase progradation complexes of grain shoal and reef-shoal deposited, such as the thick reef-shoal deposits in Mishrif_1 member in Well W-4 and W-5, and the regional inter-shoal channel deposits in Well W-6. Slopes and basin facies deposited in the western part beyond Well W-1 (Fig. 10A). In the SQ2 period, the sedimentary facies in the research area are still controlled by the regression environment, and the platform margins migrated to the east along the Well W-1 to W-10. The open platform facies grain shoal and inter-shoal hollow mainly developed in the

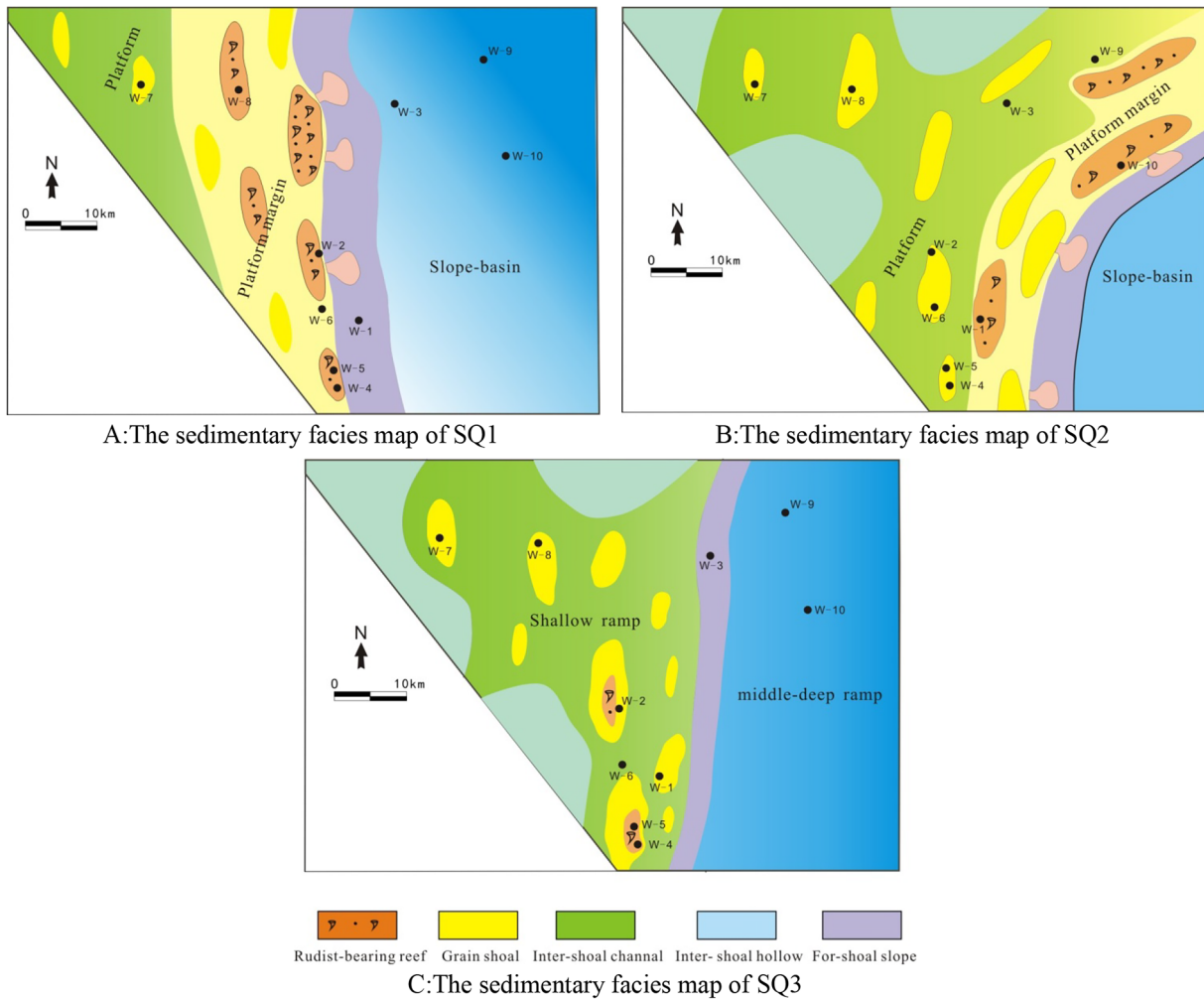
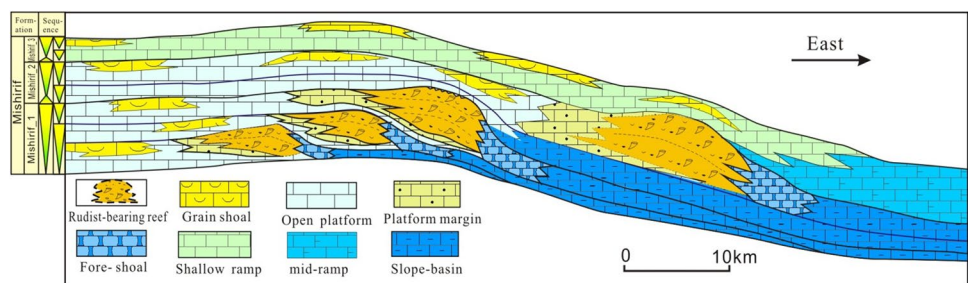


Fig. 10 The sedimentary facies map of three third-order sequence in Mishrif Formation in study area. **a** The sedimentary facies map of SQ1. **b** The sedimentary facies map of SQ2. **c** The sedimentary facies map of SQ3

Fig. 11 Profile of evolution model and distribution of Sedimentary facies in Mishrif Formation



western area. In the east part of study area, slope-basin facies deposited (Fig. 10B). In SQ3 period, the study area was dominated by ramp. Shallow ramp developed in the

central and west area, with grain shoals and channels sediments deposited. For example, grain shoal facies have been drilled in many wells such as Well W-4, W-5, and W-8.

To the east of Well W-3, the SQ3 of Mishrif Formation is mainly middle-deep ramp sediments (Fig. 10C).

Discussion

Porosity and permeability in the reservoirs

This study shows that reservoirs with good physical properties and large thickness are widely distributed in the Mishrif Formation in the Arabic basin (Aqrawi et al. 2010; Deng et al. 2016; Gao et al. 2013). The main types of pore space include intergranular pores and dissolution pores in rudist-bearing reefs and grain shoals in the Mishrif Formation (Fig. 3a, b). The dissolved pores also include intragrain dissolved pores and intergranular dissolved pores (Fig. 3b, h). These two kinds of dissolved pores are important pore types in research area.

Measurements of the core samples (214 samples from 3 wells) show that the porosity of the limestone in Mishrif Formation is about 6.9–37.9% with an average value of 20.36%, while the permeability is about $0.02\text{--}2054 \times 10^{-3} \mu\text{m}^2$ with an average value of $64.73 \times 10^{-3} \mu\text{m}^2$. Figure 12 shows that the reservoir porosity of Mishrif Formation is mainly distributed from 10 to 30%, while the permeability is $1\text{--}100 \times 10^{-3} \mu\text{m}^2$

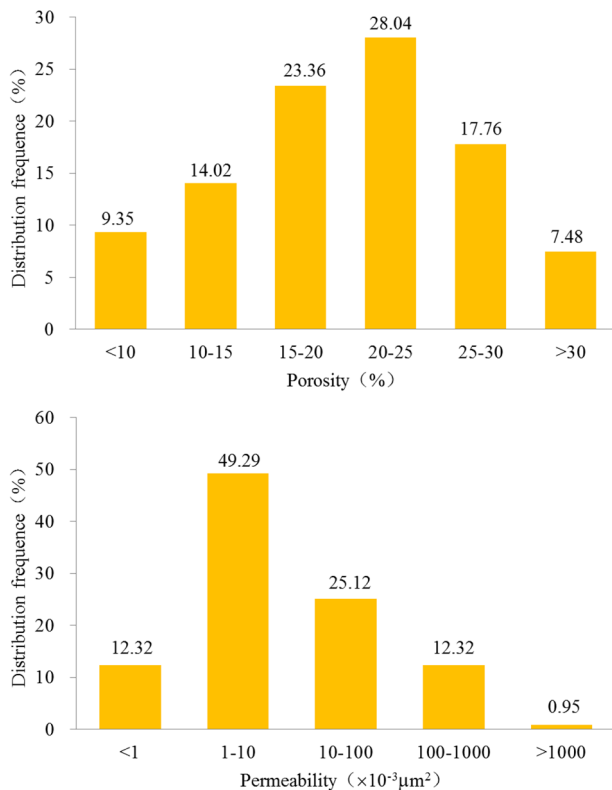


Fig. 12 Frequency distribution of the porosity and permeability of Mishrif Formation

in which exceed 13% of data is bigger than $100 \times 10^{-3} \mu\text{m}^2$, indicating medium–high porosity and medium–high permeability reservoirs in the Mishrif Formation.

Control of Sedimentary facies on reservoir quality

Sedimentary facies play an important role in controlling properties of carbonate reservoir. Previous studies on the Mishrif reservoirs in Mesopotamia Basin have concluded that pores developed well in the high-energy facies belt, such as rudist-reef, grain shoal, while inter-shoal hollows, Fore-shoal slope and middle-deep ramps usually showed poor porosity. They formed in weak water body with high lime mud content, and the pore spaces were destroyed during compaction and cementation (Fig. 3g; Wang et al. 2016; Li et al. 2020a, b). Figure 13 shows that the rudist-bearing reef and grain shoal reservoirs have the best physical properties.

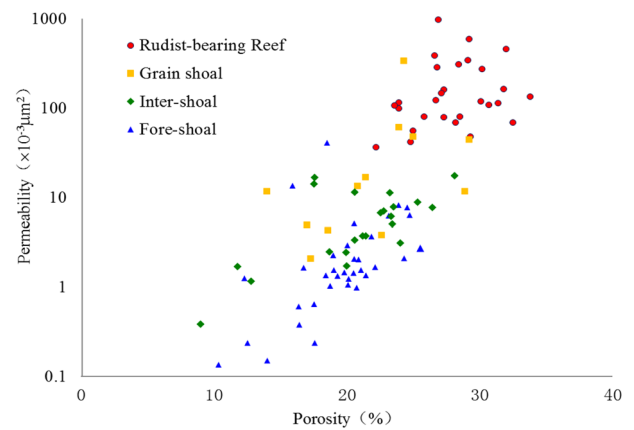


Fig. 13 Porosity and permeability classification of different sedimentary facies in Mishrif Formation

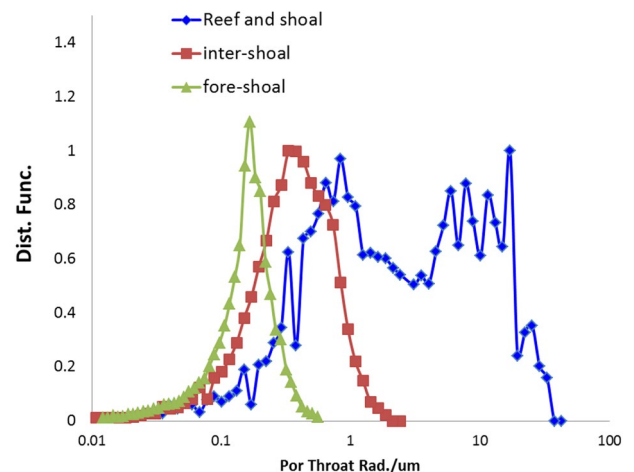


Fig. 14 Porosity throat diameter distribution of different sedimentary facies in Mishrif Formation

Average porosity of these reservoirs is over 20%, and the average permeability is over $20 \times 10^{-3} \mu\text{m}^2$. On the contrast, the inter-shoal and fore-shoal slope reservoirs also have average porosity of about 20%, but the average permeability is generally below $10 \times 10^{-3} \mu\text{m}^2$, or even below $1 \times 10^{-3} \mu\text{m}^2$. The main reason for this great discrepancy is different bioclasts and the lime mud content controlled by water energy. In the high-energy facies, high-energy water body resulted in great biological prosperity which become a big supply of framework and bioclasts, developing rudstone and grainstone with pores and throats as large as 1–10 μm (Fig. 14), while in the inter-shoal hollows and slope facies, the energy of the water body is weak, and the diameter of pores and throats is 0.1–1 μm , resulting in poor reservoir permeability (Fig. 14). In addition, in the high-energy facies, sparry cementation and strong dissolution developed due to the fresh water leaching in the syn-sedimentary stage (Fig. 3h; Li 2013; Zeng et al. 2010; Fang and Hou 2013). On the contrast, in inter-shoal and fore-shoal slope reservoirs, high mud content and strong cemented and filling in the burial

process led to the filling or disappearance of pore spaces (Fig. 3g, 15).

Sequence controls the reservoir quality

The controlling mechanisms of the Mishrif reservoirs by the stratigraphic sequence have been well studied in previous researches (Mahdi and Aqrabi 2014; Yu et al. 2018; Cantrell et al. 2020), for example, Mahdi and Aqrabi (2014) held that the upper part of the HST of the third-order sequence is more prone to high-energy shoal facies deposition, and the sequence boundary at the top of the HST is often exposed to undergo the dissolution (Fig. 3h). Six fourth-order sequences are formed in the carbonate platforms in the central-west of the research area, and nearly all of them are dominated by HST. This kind of sequence develops in the environment that water depth gradually gets shallower, which is favorable to form high-energy facies belts. Grain shoales and rudist-bearing reef usually develop in the middle and upper parts of HST. As shown in Fig. 16, the grain size of limestone gets

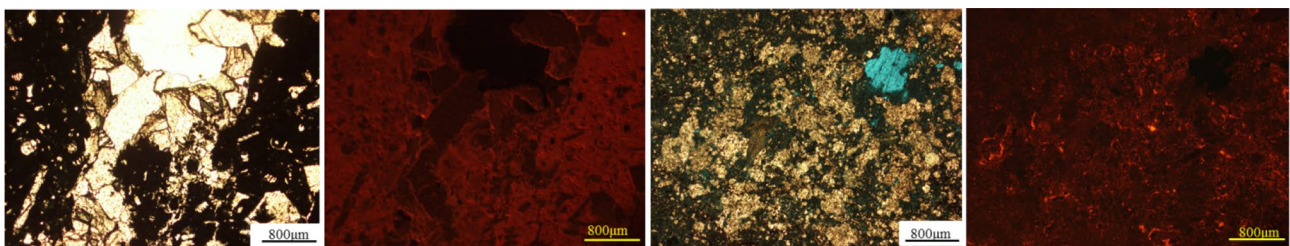


Fig. 15 Micrograph of thin sections shows diagenesis characteristics of different sedimentary facies and rocks in Mishrif Formation. **a** Wackstone, inter-shoal hollow, lime mud is dark, cemented calcite is light, W-5, 5666 ft.; **b** cathodoluminescence photo of a, lime mud or argillaceous matrix is orange, and the granular cemented calcite is

dark red; **c** Mudstone, fore-shoal slope, lime mud is dark, Recrystallized calcite is light, W-3, 5760 ft.; **d** Cathodoluminescence photo of c, lime mud or argillaceous matrix is dark red, and the granular recrystallized calcite is orange)

Fig. 16 Distribution characteristics of reservoirs in WE cross-sections through the wells of Mishrif Formation

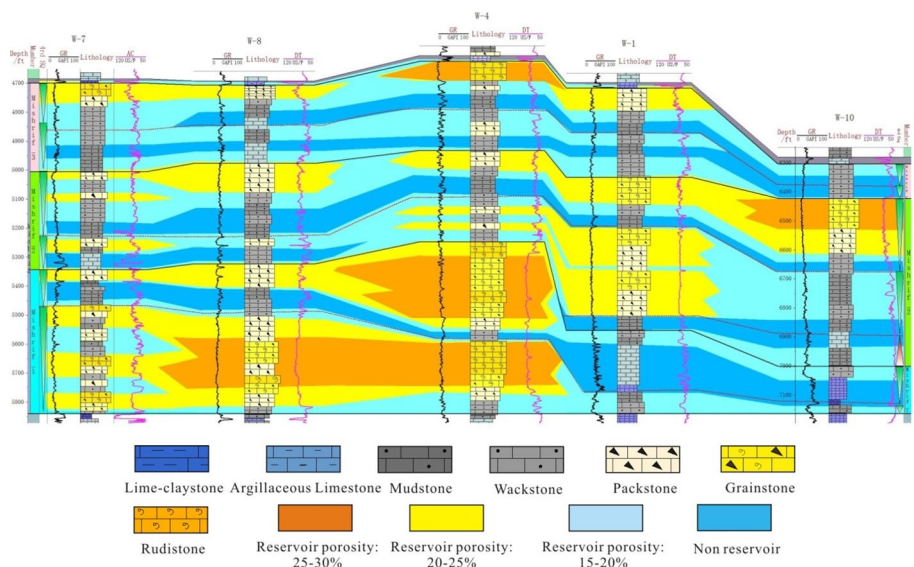
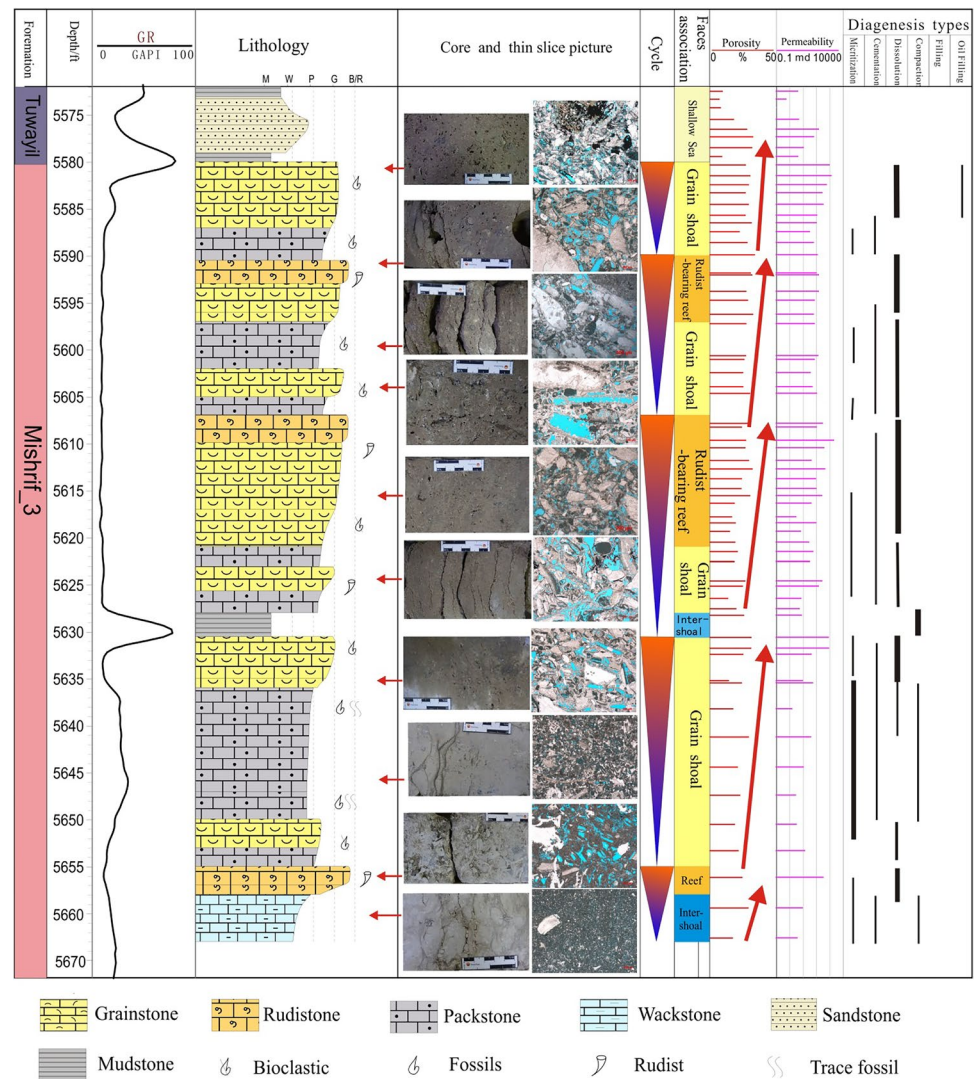


Fig. 17 Lithology description and reservoir characteristics of core section in HST of SQ3, top of Mishrif Formation in well W-5



coarser upward in each HST in well W-1 and W-4 gradually, which are mainly composed by packstone, grainstone, and rudstone. The values of AC curve increase upward, indicating better physical properties upward. The fourth-order sequence can be further divided into more secondary cycles, such as the upper 90 ft. of the core samples in well W-5 (Fig. 17). The grain size of the rocks in each secondary cycle also gets bigger upward with better physical properties. Moreover, the average grain size is bigger in upper cycle than that in lower cycle. Dissolution gets stronger upward in each secondary sequence, and martensitic dog teeth cements develop in the edge of pores, indicating exposure and fresh water leaching in the syn-sedimentary stage at the top of each cycle (Fig. 3g). This is also an important reason for better physical properties in the middle and upper parts of each fourth-order sequence or smaller sequences.

Distribution law of reservoirs

The above analysis shows that the distribution of the Mishrif reservoirs is controlled by sedimentary facies and cycle types in the sequence framework, as well as the diagenesis. In general, high-quality reservoirs are mainly distributed in the middle and upper parts of the HST cycles (Fig. 16). During these periods, the platform facies deposited above the wave base with high energy, forming coarse sediments such as bio-reef and grain shoal with low argillaceous content and abundant primary pores. High-energy facies belts such as platform margins and shallow ramp grain shoal experienced high frequency of short-term exposure and fresh water leaching, resulting in good development of dissolution pores (Fig. 16).

Vertically, two forth-order sequence of HSTs deposit in Mishrif_1 member, in which reef-shoals appear in large scale and thickness, and reservoir spaces develop well. The total thickness of the grain shoals and rudist-bearing reefs in the platform margin, such as Well W-4, reaches 500 ft., and average porosity is 25–30%, while reservoirs are very poor in the fore-shoal and slope facies. Two HST sequences deposit in the Mishrif_2 member with similar platforms and facies belts to that of the Mishrif_1 member, but its location migrates to the eastern part. Two sets of high-energy grain shoal or rudist-reef reservoirs develop in the platform margin. The thickness of reservoirs in Well W-1 reaches 400 ft., with average porosity over 20%. The open platform in the east also has some good reservoirs. Such as Well W-8, the total thickness of grain shoal and inter-shoal channel reservoir reaches 120 ft., with average porosity of 20–25%. Ramp reservoirs develop limited in Mishrif_3 member. In Ssq5 sequence, reservoirs are not developed well, while in the upper HST reservoirs develop well. For example, in Well W-5 the thickness of rudist-bearing reef and grain shoal reservoirs reaches 70 ft. (Fig. 17), and the average porosity is 25%. On the contrast, the thickness of inter-shoal channel and hollow reservoirs is only 40–60 ft., with average porosity of 15–20%.

Implications for petroleum exploration

Mishrif Formation in the Middle East is important hydrocarbon reservoirs. It is a high-quality petroleum system associating with underlying shilaif source rocks (Azzam and Taher 1993), and many big oil and gas fields have been found in the East and south Arab basin. Three third-order sequences of Mishrif Formation in the study area developed open platform, platform margin and shallow ramp facies respectively, and identified favorable facies associations such as rudist-bearing reef, grain shoal and inter-shoal channel, which have good physical properties and large distribution area. At present, oil has been found in the reef and shoal reservoirs in upper HST of SQ3 sequence (Fig. 3i). However, SQ1 and SQ2 sequences developed also thick high-quality reservoirs in large platform margin, and formed a good reservoir cap combination with the upper transgression or early low-energy facies belt of HST, which is an important potential area for oil and gas exploration in the future (Fig. 16). In particular, platform margin facies of SQ2 is closer to the source rock of shilaif basin in the East. The argillaceous limestone or claystone non-reservoir cap are well developed, therefore, this set of reservoir cap rock combination is very conducive to oil and gas accumulation, and a large reef-shoal oil and gas reservoir is expected to be found.

Conclusion

- (1) The reservoirs in Mishrif Formation are mainly composed of rudstone, grainstone, and packstone, and five types of facies associations are recognized, including rudist-bearing reef, grain shoal, inter-shoal channel/hollow, and fore-shoal slope. The reservoir spaces are mainly composed of rudist framework pores and dissolved pores. Generally, the reservoirs show high-porosity and medium–high permeability.
- (2) The Mishrif Formation can be divided into three third-order sequences and six forth-order sequences. The distribution and evolution of sedimentary facies are controlled by the internal cycles of third-order sequences and sea level change. The six forth-order sequences are dominated by HST, resulting in rimmed platforms in the early-middle stage and ramp in the late stage. Multi-phase HST form large-scale rudist-bearing reef and grain shoal with large thickness in open platform, platform margin and shallow ramp, laying foundation for the formation of large-scale reservoirs.
- (3) Favorable reservoirs in Mishrif Formation mainly develop in the middle and late stages of HST, influenced by the sedimentary facies belts and favorable diagenesis. The high-energy reef-shoal and syn-sedimentary exposed dissolution are keys to the formation of high-quality reservoirs.

Acknowledgements The primary data and research process used in this paper are supported and guided by Abu Dhabi Project of Middle East Company, PetroChina.

Data Availability Statement Data is not available for confidential reasons.

References

- Ali MY, Watts AB, Searle MP (2013) Seismic stratigraphy and subsidence history of the United Arab Emirates (UAE) rifted margin and overlying foreland basins. In: Hosani KA, Roure F, Ellison R, Lokier S (eds) *Lithosphere dynamics and sedimentary basins: the arabian plate and analogues*. Springer, pp 127–143
- Ali MY, Watts AB (2009) Subsidence history, gravity anomalies and flexure of the United Arab Emirates (UAE) foreland basin. *GeoArabia* 14:17–44
- Alsharhan AS (1995a) Sedimentology and depositional setting of the Late Cretaceous Fiqa Formation in the United Arab Emirates. *Cretac Res* 16:39–51
- Alsharhan AS (1995b) Facies variation, diagenesis, and exploration potential of the cretaceous rudist-bearing carbonates of the Arabian gulf. *AAPG Bull* 79(4):531–550
- Amer JAK (2015) The Mishrif, Yamama, and Nahr Umr reservoirs petroleum system analysis, Nasiriya oilfield, southern Iraq. *Arab J Geosci* 8(2):781–798

- Aqrabi AAM, Thehni GA, Sherwani GH et al (1998) Mid-cretaceous rudist-bearing carbonates of the Mishrif Formation: an important reservoir sequence in the Mesopotamian basin, Iraq. *J Pet Geol* 21(1):57–82
- Aqrabi AAM, Goff JC, Horbury A et al (2010) The petroleum geology of Iraq. Scientific Press, Beaconsfield, p 424
- Azzam IN, Taher AK (1993) Sequence stratigraphy and source rock potential of middle cretaceous (upper Wasia Group) in West Abu Dhabi. *SPE 25577:475–487*
- Bian CS, Li YX, Lv MS, et al. (2022) Sedimentary evolution model and sedimentary facies distribution of carbonaterocks: case study of Mishrif Formation in northeast Rub Khali Basin. *Nat Gas Geosci* 33(4):1–11 (in Chinese)
- Cantrell DL, Shah RA, Ou J et al (2020) Depositional and diagenetic controls on reservoir quality: Example from the upper Cretaceous Mishrif Formation of Iraq. *Mar Pet Geol* 118:1–34
- Deng Y, Guo R, Tian ZY et al (2016) Geologic features and genesis of the barriers and intercalations in carbonates: a case study of the Cretaceous Mishrif Formation, West Qurna oil field, Iraq. *Pet Explor Dev* 43(01):140–148 (in Chinese)
- Du JH, Zou CN, Xu CC et al (2014) Theoretical and technical innovations in strategic discovery of a giant gas field in Cambrian Longwangmiao Formation of central Sichuan paleo-uplift, Sichuan basin. *Petrol Explor Dev* 41(3):268–277 (in Chinese)
- Dunham RJ (1962) Classification of carbonate rocks according to depositional texture. In: Ham WE (ed) Classification of carbonate rocks. AAPG Memoir 1, pp 108–121
- Ehrenberg SN (2019) Petrophysical heterogeneity in a lower cretaceous limestone reservoir, onshore Abu Dhabi, United Arab Emirates. *AAPG Bull* 103:527–546
- Ehrenberga SN, Zhanga J, Gomesb JS (2020) Regional variation of permeability in Thamama-B reservoirs of Abu Dhabi. *Mar Pet Geol* 116:1–15
- Fang SX, Hou FH (2013) Diagenesis of carbonate rocks. Geological Publishing Press (in Chinese)
- Flugel E (2006) Microfacies of carbonate rocks (Ma Yongsheng, trans). Beijing: Geological Publishing House, pp 628–696
- Gao JX, Tian CB, Zhang WM et al (2013) Characteristics and genesis of carbonate reservoir of the Mishrif Formation in the Rumaila oil field, Iraq. *Acta Pet Sin* 34(5):843–852 (in Chinese)
- Hajikazemi E, Aasm IS, Coniglio M (2010) Subaerial exposure and meteoric diagenesis of the Cenomanian-Turonian upper Sarvak Formation, southwestern Iran. *Geol Soc Lond Spec Publ* 330:253–272
- Hong HT, Wang YG, Yang TQ et al (2008) Sedimentary facies of Changxing formation and distribution of organic reef gas reservoirs in northern Sichuan basin. *Nat Gas Ind* 28(1):38–41 (in Chinese)
- Jean PM, Jean B, Salim AM (1998) A platform-to-basin transition for lower Aptian carbonates (Shuaiba Formation) of the northeastern Jebel Akhdar (Sultanate of Oman). *Sediment Geol* 119(3):297–309
- John G, Zuwaina AR (2014) Depositional facies and platform architecture of microbialite-dominated carbonate reservoirs, Ediacaran-Cambrian Ara Group, Sultanate of Oman. *AAPG Bull* 98:1453–1494
- Li HT (2013) Diagenesis and characteristics of reservoir in the member 3 of the lower triassic Feixianguan formation in Heba gas field. *Acta Pet Sin* 02:263–271 (in Chinese)
- Li FF, Guo R, Liu LF et al (2020a) Heterogeneity genesis of limestone reservoirs of cretaceous Mishrif Formation in M oilfield, Iraq. *J Earth Sci Environ* 42(3):297–312 (in Chinese)
- Li FF, Guo R, Yu YC et al (2020b) Sedimentary characteristics and control in reservoirs in the cretaceous Mishrif Formation, M oilfield, Iraq. *Acta Sedimentol Sin* 38(5):1076–1087 (in Chinese)
- Mahdi TA, Aqrabi AAM (2014) Sequence stratigraphic analysis of the mid-cretaceous Mishrif Formation, southern Mesopotamian basin. *IRAQ J Petrol Geol* 37(3):287–312
- Mahdi TA, Aqrabi AAM, Horbury AD et al (2013) Sedimentological characterization of the Mid-Cretaceous Mishrif reservoir in southern Mesopotamian Basin, Iraq. *Georabia* 18(1):139–174
- Malte SST, Parente M. Chronostratigraphy of campanian–maastrichtian platform carbonates and rudist associations of salento (apulia, Italy). *Cretaceous Research*, 2008a, 29(1):0–114
- Malte SST, Parente M (2008b) Chronostratigraphy of campanian–maastrichtian platform carbonates and rudist associations of salento (Apulia, Italy). *Cretaceous Res* 29(1):0–114
- Mazeel MA (2012) Hydrocarbon reservoir potential estimated for Iraq bid round block. *Oil Gas J*
- Mohammed JA (2020) Microfacies analysis and depositional development of Shuaiba formation in the West Qurna oil field, Southern Iraq. *Model Earth Syst Environ*, pp 1–11
- Ni Xi F, Chen HD, Tian JC et al (2007) Sedimentary framework of Changxing-Feixianguan formations and its control on reservoiring in northeastern Sichuan basin. *Oil Gas Geol* 28(4):458–465 (in Chinese)
- Paola R, Andrea O, Ornella B, et al (2010) Zempolich. Depositional setting and diagenetic processes and their impact on the reservoir quality in the late Viséan–Bashkirian Kashagan carbonate platform (Pre-Caspian Basin, Kazakhstan). *AAPG Bull* 94(9):1313–1348
- Philip JM, Airaud CC (1991) The demise of the rudist-bearing carbonate platforms at the cenomanian/turonian boundary: a global control. *Coral Reefs* 10(2):115–125
- Philippe L, François F, John JGR et al (2014) Diagenetic patterns and pore space distribution along a platform to outer-shelf transect (Urgonian limestone, Barremian-Aptian, SE France). *Sed Geol* 306:1–23
- Sharland P R, Archer R, Casey D M, et al. (2001) Arabian plate sequence stratigraphy sequence. Bahrain: Gulf PetroLink, pp 10–100
- Taghavi AA, Mork A, Emadi MA (2006) Sequence stratigraphically controlled diagenesis governs reservoir quality in the carbonate Dehloran Field, southwest Iran. *Pet Geosci* 12:115–126
- Vail PR (1988) Sequence stratigraphy workbook, fundamentals of sequence stratigraphy. In: AAPG Annual convention short course, pp 217–259
- Van B, Razin F, Homewood P et al (2002) Stratigraphic organization of carbonate ramps and organic intrashelf basins: Natih Formation (middle Cretaceous) of northern Oman. *AAPG Bull* 86:21–54
- Wagoner JCV (1995) Sequence stratigraphy: an integrated technique for exploration and exploitation, part I: concepts and well log, core, and outcrop examples. *Seg Techn Progr Expand Abstr* 14(1):1521
- Wang J, Guo R, Zhao LM et al (2016) Geological features of grain bank reservoirs and the main controlling factors: a case study on Cretaceous Mishrif Formation, Halfaya oilfield, Iraq. *Petrol Explor Dev* 43(3):367–377 (in Chinese)
- Wilson JL (1975) Carbonate facies in geologic history. Springer, New York
- Yu YC, Sun LD, Song XM et al (2018) Sedimentary diagenesis of rudist shoal and its control on reservoirs: a case study of Cretaceous Mishrif Formation, H Oilfield, Iraq. *Petrol Explor Dev* 45(06):89–101 (in Chinese)
- Zeng DM, Wang XZ, Shi X et al (2010) Characteristic and reservoir property of the Leikoupo formation of middle Triassic in

- northwestern Sichuan Basin. *Acta Sedimentol Sin* 28(1):42–49 **(in Chinese)**
- Zhang JL (2017) Carbonate sequence sedimentary evolution and control of sea level: a case study of Ordovician in the Gucheng area, Tarim basin. *Nat Gas Ind* 1:46–53 **(in Chinese)**
- Zhao ZJ (2015) Indicators of global sea-level change and research methods of marine tectonic sequence: take Ordovician of Tarim Basin as an example. *Acta Pet Sin* 36(3):262–273 **(in Chinese)**
- Ziegler MA (2001) Late Permian to Holocene paleofacies evolution of the Arabian Plate and its hydrocarbon occurrences. *GeoArabia* 6(3):445–504
- Zou CN, Du JH, Xu CC et al (2014) Formation, distribution, resource potential and discovery of the Sinian-Cambrian giant gas field, Sichuan Basin, SW China. *Petrol Explor Dev* 41(3):278–293 **(in Chinese)**

Publisher's Note Springer Nature remains neutral with regard to jurisdictional claims in published maps and institutional affiliations.

Springer Nature or its licensor holds exclusive rights to this article under a publishing agreement with the author(s) or other rightsholder(s); author self-archiving of the accepted manuscript version of this article is solely governed by the terms of such publishing agreement and applicable law.